

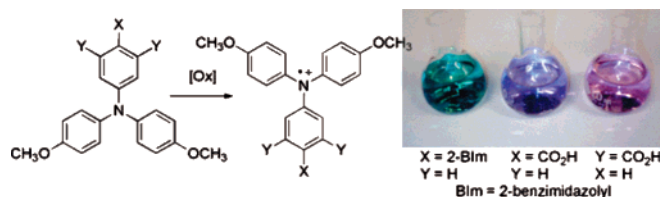
## Synthesis and Oxidation of Triarylamine Derivatives Bearing Hydrogen-Bonding Groups

Hidenori Murata<sup>†</sup> and Paul M. Lahti\*

Department of Chemistry, University of Massachusetts,  
Amherst, Massachusetts 01003

lahti@chem.umass.edu

Received February 15, 2007



Hydrogen-bonding triarylamines, 4-(*N,N*-bis(4-methoxyphenyl)amino)benzoic acid (**TPA1**), 5-(*N,N*-bis(4-methoxyphenyl)amino)isophthalic acid (**TPA2**), and *N*-(4-(1*H*-benzimidazol-2-yl)phenyl)-*N,N*-bis(4-methoxyphenyl)amine (**BImTPA**), were synthesized as radical cation precursors. **TPA1** and **TPA2** are readily p-doped by AgSbF<sub>6</sub> to give highly persistent radical cations. Poor solid-state spin yields of the radical cation from **BImTPA** may be due to spin delocalization.

Cationic doping of triarylamines is an important strategy in organic-based magnetic materials.<sup>1</sup> Hydrogen-bonding interactions are useful to help assemble molecules in the solid state with some degree of control, to try to control intermolecular exchange between unpaired electrons.<sup>2</sup> However, hydrogen-bonded assembly has not been much used to our knowledge in p-dopable triarylamines, although 4-(*N,N*-bis(4-methoxyphenyl)amino)benzoic acid, **TPA1**, was made as a synthetic intermediate for studies of photoactive and luminescent organometallic complexes.<sup>3</sup> To our knowledge, the solid-state hydrogen bonding and chemical doping behavior of **TPA1** has not been studied. This paper describes the oxidation of three hydrogen-bonding triphenylamines: **TPA1**, 5-(*N,N*-bis(4-methoxyphenyl)amino)isophthalic acid (**TPA2**), and *N*-(4-(1*H*-benzimidazol-2-yl)phenyl)-*N,N*-bis(4-methoxyphenyl)amine (**BImTPA**). **TPA1** and **TPA2** were crystallographically characterized, and all three were p-doped in both solid state and solution to give highly persistent

radical cations that were studied by magnetic susceptibility, UV-vis, and electron spin resonance spectroscopy.

Scheme 1 shows the methods used to make the triarylamines. **TPA1** was made by Pd<sub>2</sub>(dba)<sub>3</sub>-catalyzed coupling of *N,N*-bis(4-methoxyphenyl)amine (**BMPA**) with methyl 4-iodobenzoate, followed by hydrolysis of the obtained crude ester. **TPA2** was made analogously by coupling **BMPA** with dimethyl 5-iodoisophthalate, followed by hydrolysis of the crude diester. **TPA1** was then condensed with 1,2-diaminobenzene to give **BImTPA**. The product amines were all satisfactorily characterized by <sup>1</sup>H NMR, <sup>13</sup>C NMR, FTIR, and elemental composition.

Addition of SbCl<sub>5</sub> or AgSbF<sub>6</sub> (Figure 1) to dichloromethane solutions of the triarylamines immediately gave deep colors associated with the corresponding radical cations. **TPA1-rc** was violet, **TPA2-rc** red-purple, and **BImTPA-rc** green. The associated UV-vis maxima were 356, 577, and 785 nm for **TPA1-rc**, 365, 520, and 793 nm for **TPA2-rc**, and 290, 365, 401, ~630 (shoulder), and 777 nm for **BImTPA-rc**. The colors persisted for days in air. The similarity of the **TPA1-rc** and **TPA2-rc** absorption spectra is consistent with their chromophoric similarity. The transient spectroscopy of photooxidation and the chemical oxidation of **TPA1** with Br<sub>2</sub> show absorption bands at 750 and 590 nm that are attributed<sup>3</sup> to the radical cation; these are in good agreement with the present results. Part of the spectrum of **BImTPA-rc** is significantly perturbed by comparison, with doubling of a peak found around 350–360 nm in the other two systems (new peak at ~400 nm) and a red shift of the band at about 500–600 nm to about 630 nm. However, the lowest energy, strongest peak in all is at 780–800 nm (~1.55 eV).

Table 1 summarizes solution ESR hyperfine couplings for the radical cations generated by AgSbF<sub>6</sub> oxidation of TPA solutions in dichloromethane at room temperature. **TPA1-rc** and **TPA2-rc** show hyperfine coupling (hfc) from the aryl protons, but any analogous hfc in **BImTPA-rc** was masked by line broadening, despite attempts in several solvents in the temperature range of 100–300 K. The ESR spectra of samples produced by SbCl<sub>5</sub> vapor oxidation were essentially the same. Under no conditions or solvents attempted were ESR peaks observed that were clearly attributable to triplet state radical pairs, either in fluid solution or at 77 K in frozen solution.

Numerous attempts to crystallize **BImTPA** failed to yield single crystals of sufficient quality for X-ray diffraction (XRD) analysis. Its high melting point suggests strong intermolecular interactions. FTIR shows a broad NH stretching envelope over 2800–3100 cm<sup>-1</sup> that suggests NH...N hydrogen bonding (NH...N chain formation is common for 2-substituted benzimidazoles). **TPA1** and **TPA2** crystallize well from chloroform/methanol and were readily analyzed by single-crystal XRD.

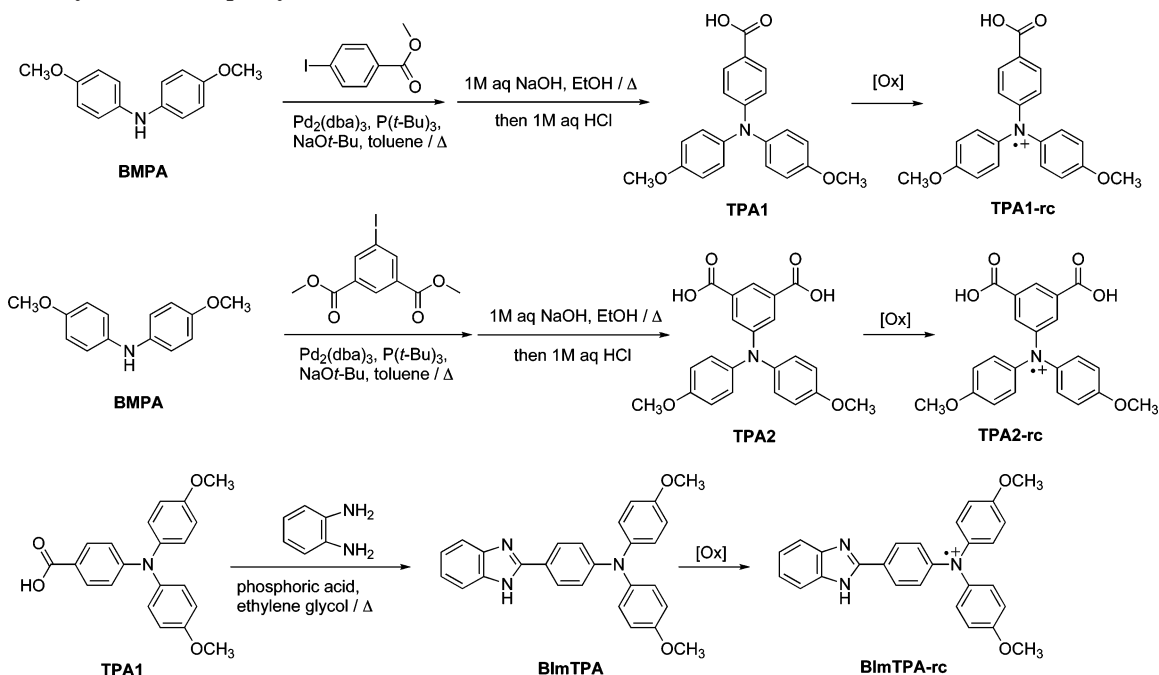
<sup>†</sup> Present address: Department of Pure & Applied Chemistry, Faculty of Science & Technology, Tokyo University of Science, Noda, Chiba 278-8510, Japan.

(1) (a) Ito, A.; Ino, H.; Matsui, Y.; Hirao, Y.; Tanaka, K. *J. Phys. Chem. A* **2004**, *108*, 5715. (b) Bushby, R. J.; Gooding, D. *J. Chem. Soc., Perkin Trans. 2* **1998**, 1069. (c) Tyutylkov, N.; Baumgarten, M.; Dietz, F. *Chem. Phys. Lett.* **2002**, *353*, 231. (d) Stickly, K. R.; Blackstock, S. C. *J. Am. Chem. Soc.* **1994**, *116*, 11576. (e) Selby, T. D.; Blackstock, S. C. *J. Am. Chem. Soc.* **1999**, *121*, 7152. (f) van Meurs, P. J.; Janssen, R. A. *J. Org. Chem.* **2000**, *65*, 5712. (g) Okada, K.; Imakura, T.; Oda, M.; Murai, H.; Baumgarten, M. *J. Am. Chem. Soc.* **1996**, *118*, 3047. (h) Sato, K.; Yano, M.; Furuichi, M.; Shiomi, D.; Takui, T.; Abe, K.; Itoh, K.; Higuchi, A.; Katsuma, K.; Shirota, Y. *J. Am. Chem. Soc.* **1997**, *119*, 6607. (i) Murata, H.; Takahashi, M.; Namba, K.; Takahashi, N.; Nishide, H. *J. Org. Chem.* **2004**, *69*, 631. (j) Fukuzaki, E.; Nishide, H. *J. Am. Chem. Soc.* **2006**, *128*, 996.

(2) (a) Veciana, J.; Cirujeda, J.; Rovira, C.; Molins, E.; Novoa, J. *J. Solid State Chem.* **2001**, *159*, 440–450. (b) Maspocho, D.; Domingo, N.; Ruiz-Molina, D.; Wurst, K.; Tejada, J.; Rovira, C.; Veciana, J. *Compt. Rend. Chim.* **2005**, *8*, 1213. (c) Lahti, P. M. Magneto-structural Correlations in  $\pi$ -Conjugated Nitroxide-based Radicals: Hydrogen-bonds and Related Interactions in Molecular Organic Solids. In *Carbon-based magnetism: An overview of the magnetism of metal-free carbon-based compounds and materials*; Makarova, T., Palacio, F., Eds.; Elsevier: Amsterdam, 2006; pp 23–52.

(3) (a) Baranoff, E.; Dixon, I. M.; Collin, J.-P.; Sauvage, J.-P.; Ventura, B.; Flamigni, L. *Inorg. Chem.* **2004**, *43*, 3057. (b) Flamigni, L.; Baranoff, E.; Collin, J.-P.; Sauvage, J.-P. *Chem.—Eur. J.* **2006**, *12*, 6592.

## SCHEME 1. Synthesis of Triphenylamines and Derived Radical Cations



**TPA2** also crystallizes well from THF, but this solvent is incorporated into the lattice.

Powdered **TPA1**, **TPA2**, or **BImTPA** exposed to  $\text{SbCl}_5$  vapor for 24 h turned blue-black, blue-black, and green-black, respectively. The oxidized samples remained visually unchanged after exposure to room air for weeks. Measurements of the vapor-doped paramagnetic susceptibilities of powdered **TPA1** and **TPA2** showed 28 and 12% of the theoretical moments expected if all molecules yielded  $S = 1/2$  spin units (Supporting Information). Single crystals of **TPA1** and **TPA2** that were doped for 24 h showed pale yellow interiors when broken, proving that extensive diffusive doping does not occur readily from the vapor phase.

By comparison, dichloromethane solutions of **TPA1**, **TPA2**, or **BImTPA** treated with  $\text{AgSbF}_6$  immediately turned deeply colored and could be precipitated into hexane to give dark colored powders that were readily studied by paramagnetic susceptibility (Figure 2). The data indicate 59, 79, and 4% yields of spin units from this procedure, relative to a theoretical value of  $0.375 \text{ emu}\cdot\text{K}/\text{Oe}\cdot\text{mol}$  for 100% generation of  $S = 1/2$  spin carriers, and assuming that the basic spin units are monoradical cations with  $\text{SbF}_6^-$  counterions.

Neutral **TPA1** forms crystallographic dimers, a typical motif for monocarboxylic acids.<sup>4</sup> **TPA2** forms 1-D ribbons, as is common in isophthalic acids.<sup>4</sup> In both, the aryl rings are significantly twisted relative to one another. All methoxy and some aryl groups show moderately large thermal motion ellipsoids at room temperature, but the molecules are not otherwise disordered. Although the hydrogen bonds hold the amine molecules closer together than might occur without the interaction, the crystallographic geometries found in the neutral amines appear unlikely to assist strong exchange. The closest  $\text{N}\cdots\text{N}$  distances (Supporting Information) in **TPA1** are 5.8–5.9 Å, and in **TPA2**, they are 6.74 Å, too large to allow strong, direct exchange due to direct overlap of  $\text{N}(2p)$  orbitals from the aminium radical cation centers. It seems likely that swelling of the lattice to accommodate dopant counterions would move the TPA radical cations further apart, although this was not

directly probed. However,  $\pi$ -orbital contact between aryl units could also give exchange between radical cations, given their significant spin densities delocalized from the aminium centers. In **TPA1**, the  $\pi$ -carbon *ipso* to the carboxylic acid group is only 3.52 Å from a  $\pi$ -carbon *ortho* to the acid group on a neighboring molecule. For **TPA2**, inversion symmetry gives to an antiparallel close contact of 3.36 Å between the phenyl– $\text{CO}_2\text{H}$  bonds (Supporting Information). These contacts do not provide ideal  $\pi$ -system overlap for inter-radical exchange, but modest realignment during doping could easily improve them.

UB3LYP/6-31G\* geometry optimized computations<sup>5</sup> for the three radical cations were carried out in order to evaluate further their spin delocalization and to compare to the experimental ESR hfc. Solution-phase ESR spectra of **TPA1-rc** and **TPA2-rc** show aryl C–H hyperfine coupling consistent with the computational 6–9% and (–)2–4% spin populations on the phenyl  $\pi$ -carbons *ortho* and *meta* to the aminium nitrogen, respectively. These delocalized spin density sites could provide exchange sites where close contacts between doped radical cations occur in the solid state, depending on the intermolecular contacts between molecules in the doped form.

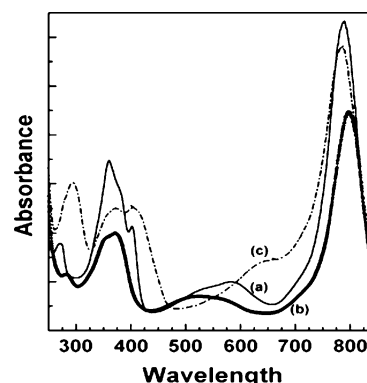


**FIGURE 1.** UV–vis spectra of radical cations from  $\text{AgSbF}_6$  oxidation of neutral amines at room temperature in dichloromethane: (a) **TPA1-rc**, (b) **TPA2-rc**, (c) **BImTPA-rc**.

TABLE 1. Solution ESR Hyperfine Coupling Constants

TPA1-rc	$a(\text{N}) = 8.58 \text{ G}$
	$a(\text{H}) = 1.37(6\text{H})$
	$a(\text{H}) = 1.00(6\text{H})$
TPA2-rc	$a(\text{H}) = 0.56(6\text{H})$
	$a(\text{N}) = 8.57 \text{ G}$
	$a(\text{H}) = 1.38(7\text{H})$
BImTPA-rc	$a(\text{H}) = 1.05(6\text{H})$
	$a(\text{H}) = 0.57(4\text{H})$
	$a(\text{N}) = 8.33 \text{ G}$

Unresolved benzimidazole hfc in **BImTPA-rc** probably gives heterogeneous line shape broadening that obscures aryl CH hyperfine in its ESR spectrum. The UB3LYP/6-31G\* computations support this, showing that  $(-)$ 1.6% of spin density is delocalized onto the benzimidazole 2-C position, 5.4% onto the imine 3-N position, and about  $(\pm)$ 1–6% onto the benzimidazole aryl carbons. The significant shifts in some UV–vis bands of **BImTPA-rc** by comparison to those of **TPA1-rc** and **TPA2-rc** also reflect electronic conjugation between the radical site and the benzimidazole group.

Vapor-phase p-doping of neat powdered **TPA1** and **TPA2** with  $\text{SbCl}_5$  gives a surface radical cation layer that persists for many weeks but does not peruse the sample bulk, as explained above. At low temperatures, the  $\chi T(T)$  data for vapor p-doped samples show weak antiferromagnetic (AFM) exchange (Supporting Information), so the amount of surface doping is sufficient to give exchange interaction between radical cation sites by proximity. The neutral amines **TPA1** and **TPA2** are held in sufficient proximity in their crystal lattices that their doped forms could show small to modest intermolecular exchange interaction, assuming that the dimer and chain hydrogen-bond motifs are maintained after doping.

Solution-phase doping of **TPA1** and **TPA2** with  $\text{AgSbF}_6$  gives precipitated products with much higher spin yields. The exchange behaviors of these products are not necessarily related to those of the vapor-doped TPA samples, but they do also show  $\chi T(T)$  downturns at lower temperature, indicating AFM exchange interactions, and their  $1/\chi(T)$  versus  $T$  plots give Weiss constants of  $(-)$ 6.3 and  $(-)$ 2.6 K, respectively. Solid powder samples and solutions of the radical cations generated this way are highly persistent under ambient conditions and retain their characteristic deep coloration for over a year at  $-30^\circ\text{C}$ . The carboxylic acid units at the *para* (**TPA1-rc**) and both *meta* (**TPA2-rc**) positions of the non-methoxylated phenyl rings are apparently effective steric blockading groups, limiting reactions such as radical dimerization or oxygen trapping. However, these samples were not readily subjected to further purification or recrystallization. Attempts at slow evaporation from dichloromethane and slow diffusion of hexane into dichloromethane did not yield crystals of sufficient quality for single-crystal X-ray diffraction analysis, so detailed magnetostructural analysis of the antiferromagnetic interactions in the radical cations is not possible at this time, but hydrogen bonding in these systems is a major part of bringing the molecules closer together in the neutral TPA systems and is likely to be an important contributor to holding the radical cations in proximity in the neat solids.

Although **BImTPA** gives radical cations in amounts readily detected by ESR from both vapor and solution oxidation

techniques, magnetic studies of products from both methods showed disappointingly poor spin yields of only 4–5%. Solutions of this radical cation also are not as color-persistent as those from **TPA1** and **TPA2**. The radical cation **BImTPA-rc** is formed to a significant extent, however, based on the spectroscopic results described above, as well as cyclic voltammetry (CV). CV in  $\text{CHCl}_3$  shows roughly quasi-reversible behavior, with  $E^{\circ'}$  values for  $(n, +)$  of 720, 640, and 560 mV at 10 mV/s sweep rate for **TPA1**, **TPA2**, and **BImTPA**, respectively. In order of ease of oxidation, **BImTPA** > **TPA2** > **TPA1**. Since **BImTPA** is the most easily oxidized of the triarylamines in this study, its low solid-state spin yield may be due to increased reactivity in the solid. **BImTPA-rc** has spin delocalization onto its benzimidazole unit based on its UV and ESR spectroscopy, as well as the computational modeling results. This could cause solid-state dimerization and other reactions with consequent loss of spin moment.

Attachment of one carboxylic acid group to a TPA leads to solid-state dimer formation, while attachment of an isophthalic acid group leads to ribbon formation, both due to directional hydrogen bonding between the carboxylic acid groups. The hydrogen bonding between carboxylic acid groups in **TPA1** and **TPA2** holds them together in motifs that were expected by analogy to other benzenoid and isophthalic acid functionalized systems. Use of benzimidazole as a hydrogen-bonding substituent did not yield diffraction quality crystals, but hydrogen-bonded chains would be expected by analogy to other benzimidazoles. Hence, hydrogen bonding does serve to bring the triarylamine units into close solid-state proximity. This has potential use for the crystal assembly of dopable organic paramagnet precursors and for bringing electron donor triarylamines into proximity with other molecules to act as energy transfer or quenching agents.

**BImTPA** exhibited only small spin yields in cationic doping experiments, with limited persistence of its radical cation solutions. This was attributed to spin delocalization in this system. Cationic doping of the carboxylic acid functionalized TPAs gives highly persistent radical cations readily characterized by solution molecular spectroscopy. Solid-state magnetic measurements of the latter radical cations show strong doping levels, with modest antiferromagnetic exchange interactions at low temperature. This high persistence of the carboxylic acid functionalized radical cation systems makes them promising as possible spin-bearing components in solid-state magnetic materials and related electronic materials.

## Experimental Section

**4-(*N,N*-Bis(4-methoxyphenyl)amino)benzoic acid (TPA1).** 4-Iodobenzoic acid methyl ester (3.43 g, 13.1 mmol) and *N,N*-bis(4-methoxyphenyl)amine<sup>6</sup> (3.00 g, 13.1 mmol) were dissolved in toluene (19.6 mL). Sodium *tert*-butoxide (1.51 g, 15.7 mmol), tri-*tert*-butylphosphine (0.318 g, 1.57  $\mu\text{mol}$ ), and tris(dibenzylideneacetone)dipalladium (0.300 g, 0.328  $\mu\text{mol}$ ) were added, and then the mixture was heated at  $100^\circ\text{C}$  for 7 h. The reaction mixture was neutralized with 1 N aqueous ammonia and extracted with chloroform. The organic layer was washed with brine and evaporated to give the crude product, which was added to 146 mL of ethanol and mixed with 146 mL of 1 M aq NaOH. The mixture was heated to reflux for 1 h and then cooled to room temperature and concentrated. The precipitate that formed was filtered. Then 182 mL of water was added, and 182 mL of 1 M aq HCl was

(4) (a) Etter, M. C. *Acc. Chem. Res.* **1990**, *23*, 120–126. (b) Bernstein, J.; Etter, M. C.; Leiserowitz, L. *Struct. Correl.* **1994**, *2*, 431–507.

(5) All computations in this paper were carried out using Spartan 2002 for Irix 6.5 by Wavefunction Inc., Irvine CA.

(6) Ma, D.; Cai, Q.; Zhang, H. *Org. Lett.* **2003**, *5*, 2453.

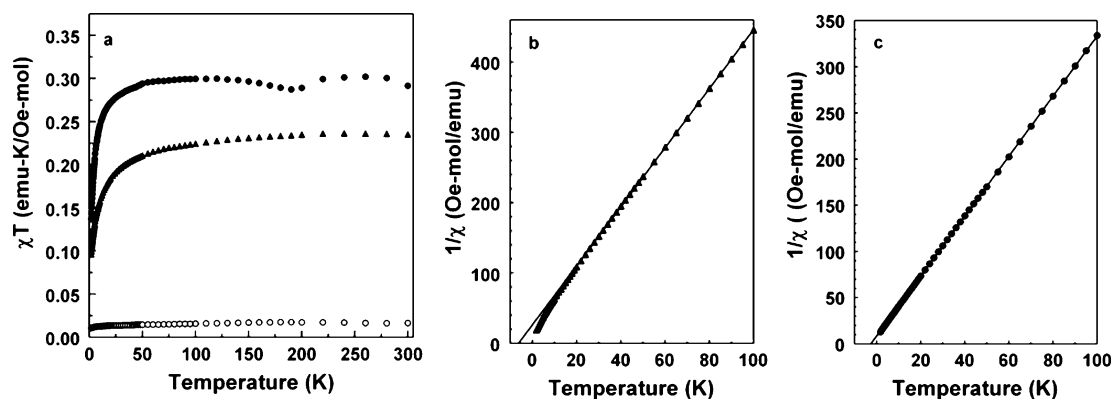


**FIGURE 2.** (a) Paramagnetic susceptibility  $\chi T$  versus temperature plots for solution doped samples of **TPA1** (▲), **TPA2** (●), and **BImTPA** (○) at 1000 Oe; (b) Curie–Weiss plot for **TPA1**; (c) Curie–Weiss plot for **TPA2**.

added dropwise while the reaction was stirred. The resulting yellow precipitate was filtered, washed with water, and dried. Chromatography of the solid (silica gel, ethyl acetate) yielded **TPA1** (2.75 g, 60%), which was recrystallized as yellow rhombi from chloroform/methanol: mp 204–206 °C;  $^1\text{H}$  NMR ( $\text{CDCl}_3$ )  $\delta$  7.85 (d, 2H,  $J = 9.0$  Hz), 7.11 (d, 4H,  $J = 9.0$  Hz), 6.87 (d, 4H,  $J = 9.0$  Hz), 6.81 (d, 2H,  $J = 9.0$  Hz), 3.81 (s, 6H);  $^{13}\text{C}$  NMR ( $\text{CDCl}_3$ )  $\delta$  171.1, 157.0, 153.4, 139.3, 131.6, 127.9, 119.0, 116.8, 115.0, 55.5; IR (KBr pellet,  $\text{cm}^{-1}$ ) 2958 (OH str), 1669 (C=O str); MS (EI,  $m/z$ ) calcd for  $\text{C}_{21}\text{H}_{19}\text{NO}_4$  349, found 349.4. Anal. Calcd for  $\text{C}_{21}\text{H}_{19}\text{NO}_4$ : C, 72.19; H, 5.48; N, 4.01. Found: C, 72.09; H, 5.39; N, 3.94. Single-crystal X-ray structural analysis results were submitted to the Cambridge Structural Database, deposition number 636280.

**5-(*N,N*-Bis(4-methoxyphenyl)amino)isophthalic acid (TPA2).** 5-Iodoisophthalic acid dimethyl ester<sup>7</sup> (2.50 g, 7.81 mmol) and *N,N*-bis(4-methoxyphenyl)amine<sup>6</sup> (1.79 g, 7.81 mmol) were dissolved in toluene (11.7 mL). Sodium *tert*-butoxide (0.901 g, 9.37 mmol), tri-*tert*-butylphosphine (0.158 g, 781  $\mu\text{mol}$ ), and tris(dibenzylideneacetone)dipalladium (0.165 g, 180  $\mu\text{mol}$ ) were added, and the mixture was heated at 100 °C for 7 h. The reaction mixture was neutralized with 1 N aq ammonia and extracted with chloroform. The organic layer was washed with brine and evaporated to give the crude product, to which was added 87 mL of ethanol then 87 mL of 1 M aq NaOH. The mixture was heated to reflux for 1 h and then cooled to room temperature and concentrated. The resulting precipitate was filtered and suspended in 108 mL of water, then 108 mL of 1 M aq HCl was added dropwise with stirring. The resulting yellow precipitate was filtered, washed with water, and dried. Chromatography of the solid (silica gel, ethyl acetate) yielded **TPA2** (2.15 g, 70%), which crystallized as yellow rhombi from chloroform/methanol: mp 304–306 °C;  $^1\text{H}$  NMR (acetone- $d_6$ )  $\delta$  8.11 (s, 1H), 7.16 (d, 4H,  $J = 8.8$  Hz), 7.69 (s, 2H), 6.97 (d, 2H,  $J = 8.8$  Hz), 3.81 (s, 6H);  $^{13}\text{C}$  NMR (acetone- $d_6$ )  $\delta$  166.1, 157.1, 149.8, 139.7, 131.8, 127.4, 123.0, 121.4, 115.1, 54.8; IR (KBr,  $\text{cm}^{-1}$ ) 2930 (OH str), 1693 (C=O str); MS (EI,  $m/z$ ) calcd for  $\text{C}_{22}\text{H}_{19}\text{NO}_6$  393, found 393.4. Anal. Calcd for  $\text{C}_{22}\text{H}_{19}\text{NO}_6$ : C, 67.17; H, 4.87; N, 3.56. Found: C, 67.04; H, 4.79; N, 3.54. Single-crystal X-ray structural analysis results were submitted to the Cambridge Structural Database, deposition number 636282 (and 636281 for a THF solvent incorporated structure).

***N*-(4-(1*H*-Benzimidazol-2-yl)phenyl)-*N,N*-bis(4-methoxyphenyl)amine (BImTPA).** A mixture of **TPA1** (200 mg, 572  $\mu\text{mol}$ ), *o*-phenylenediamine (61.9 mg, 572  $\mu\text{mol}$ ), and phosphoric acid (561 mg, 572  $\mu\text{mol}$ ) was dissolved in ethylene glycol (0.46 mL), stirred at 160 °C for 14 h under nitrogen, cooled to room temperature, and concentrated. Chromatography of the resulting solid (silica gel, ethanol) yielded **BImTPA** (96.4 mg, 40%) as a yellow powder: mp 225–226 °C;  $^1\text{H}$  NMR (methanol- $d$ )  $\delta$  7.68 (d, 2H,  $J = 6.8$  Hz), 7.37 (m, 2H), 7.03 (m, 2H), 6.92 (d, 4H,  $J = 6.8$  Hz), 6.77 (d, 2H,  $J = 6.8$  Hz), 6.69 (d, 4H,  $J = 6.8$  Hz), 3.62 (s, 6H);  $^{13}\text{C}$  NMR (methanol- $d$ )  $\delta$  156.4, 152.3, 150.4, 140.0, 127.5, 127.3,

122.3, 120.4, 118.9, 114.8, 114.4, 55.4; IR (KBr pellet,  $\text{cm}^{-1}$ ) 2930 (NH str); MS (EI,  $m/z$ ) calcd for  $\text{C}_{27}\text{H}_{23}\text{N}_3\text{O}_2$  421, found 421.5. Anal. Calcd for  $\text{C}_{27}\text{H}_{23}\text{N}_3\text{O}_2$ : C, 76.94; H, 5.50; N, 9.97. Found: C, 76.69; H, 5.60; N, 9.71.

**Oxidation of TPA1 with AgSbF<sub>6</sub>.** A solution of AgSbF<sub>6</sub> (53.9 mg, 157  $\mu\text{mol}$ ) in dichloromethane (5 mL) was added dropwise to a solution of **TPA1** (50.0 mg, 143  $\mu\text{mol}$ ) in dichloromethane (2.5 mL); the reaction instantly turned from yellow to deep violet. The solution was then filtered and evaporated to give the crude product, which was dissolved in a small amount of dichloromethane and poured into excess hexane to precipitate the radical cation as a deeply colored violet-black solid (44.2 mg, 53%) that was dried under vacuum for ESR and magnetism studies.

**Oxidation of TPA2 with AgSbF<sub>6</sub>.** A solution of AgSbF<sub>6</sub> (95.9 mg, 279  $\mu\text{mol}$ ) in dichloromethane (9 mL) was added dropwise to a solution of **TPA2** (100 mg, 254  $\mu\text{mol}$ ) in dichloromethane (2.5 mL); the reaction instantly turned from yellow to red-purple. The solution was then filtered and evaporated to give the crude product, which was dissolved in a small amount of dichloromethane and poured into excess hexane to precipitate the radical cation as a darkly purple colored solid (66.0 mg, 41%) that was dried under vacuum for ESR and magnetism studies.

**Oxidation of BImTPA with AgSbF<sub>6</sub>.** A solution of AgSbF<sub>6</sub> (17.9 mg, 52.2  $\mu\text{mol}$ ) in dichloromethane (2 mL) was added dropwise to a solution of the **BImTPA** (20 mg, 47.5  $\mu\text{mol}$ ) in dichloromethane (5 mL); the reaction instantly turned from yellow to green. The solution was then filtered and evaporated to give the crude product, which was dissolved in a small amount of dichloromethane and poured into excess hexane to precipitate the radical cation as a deeply colored green-to-black solid (17.9 mg, 57%) that was dried under vacuum for ESR and magnetism studies.

**Acknowledgment.** This work was supported by the National Science Foundation under Grant CHE-0415716. The University of Massachusetts Mass Spectrometry Facility, Nanomagnetic Characterization Facility, X-ray Structural Characterization Laboratory, and EPR Facility are also supported in part by the National Science Foundation.

**Supporting Information Available:** General methods used, crystallographic summaries for **TPA1** and **TPA2** and **TPA2·THF**, including full details in CIF format; computational spin density summaries for radical cations; solution ESR spectra and hyperfine simulations for radical cations, FTIR spectra for neutral amines; characterization NMR spectra, summary of Curie and Weiss constants from doping experiments, cyclic voltammetry for **TPA1**, **TPA2**, and **BImTPA**. This material is available free of charge via the Internet at <http://pubs.acs.org>.

JO070318A

(7) Boomgaarden, W.; Vogtle, F.; Nieger, M.; Hupfer, H. *Chem.—Eur. J.* **1999**, *5*, 345.